Slow-Light Fourier Transform Interferometer

Zhimin Shi* and Robert W. Boyd
The Institute of Optics, University of Rochester, Rochester, New York 14627 USA

Ryan M. Camacho, Praveen K. Vudyasetu, and John C. Howell
Department of Physics and Astronomy, University of Rochester, Rochester, New York 14627 USA

(Received 11 July 2007; published 11 December 2007)

We describe a new type of Fourier transform (FT) interferometer in which the tunable optical delay between the two arms is realized by using a continuously variable slow-light medium instead of a moving arm as in a conventional setup. The spectral resolution of such a FT interferometer exceeds that of a conventional setup of comparable size by a factor equal to the maximum group index of the slow-light medium. The scheme is experimentally demonstrated by using a rubidium atomic vapor cell as the tunable slow-light medium, and the spectral resolution is enhanced by a factor of approximately 100.

DOI: 10.1103/PhysRevLett.99.240801 PACS numbers: 07.60.Ly, 07.60.Rd, 42.62.Fi

Recently, there has been considerable interest in the development of slow- and fast-light techniques [1] to control the propagation velocity of light pulses through a material system. While early work concentrated on techniques to realize very large [2,3], very small [4], or even negative [5] group indices, recent work has been aimed at developing practical applications of slow-light methods [6–11]. In addition to applications in optical communication systems [1], it was recently shown that slow light can also be used to enhance the spectral sensitivity of certain types of interferometers [12–14].

Fourier transform (FT) interferometry [15] is a powerful technique that has an intrinsically high signal-to-noise ratio (SNR) and can have high resolving power. These properties have led to its many applications in biomedical engineering, metrology [16], astronomy, etc. A conventional FT interferometer [see Fig. 1(a)] is typically comprised of a fixed arm and a moving arm, both of which contain nondispersive media (typically air) with refractive index n. The length of the moving arm can be changed to achieve a variable optical delay time (ODT) $\tau = nL/c$, where L is the length difference between the two arms, and c is the speed of light in vacuum. To resolve the spectrum of an input optical field with center frequency ν, τ needs to be tuned from zero to a maximum value $\tau_{\max}$ with a step size comparable to $1/\nu$. The spectral resolution is given by $\delta\nu_{\min} = 1/(2\tau_{\max})$ [15]. To achieve a high spectral resolution, one needs a large device size [typically with the order of $c/(2n\delta\nu_{\min})$] and a large number of data acquisition steps [determined by $\nu/(2\delta\nu_{\min})$] for each measurement.

In this Letter, we propose and demonstrate a new type of FT interferometer that uses a continuously tunable slow-light medium to realize a tunable group delay between the two arms [see Fig. 1(b)]. We first develop the theory for the ideal case in which the slow-light medium has a uniform group index n_g (defined by $n_g \equiv n + \nu dn/d\nu$) and thus no group velocity dispersion over the frequency range of interest. The frequency dependence of the refractive index of such an ideal tunable slow-light medium in the vicinity of a reference frequency ν_0 is given by

$$n(\nu) \approx n(\nu_0) + \frac{n_g' \nu'}{\nu_0}, \tag{1}$$

where $\nu' \equiv \nu - \nu_0$ is the frequency detuning and $n_g' \equiv n_g - n$ is the relative group index. We assume that for such a medium n_g' can be varied continuously, for example, by changing the number density of an atomic vapor, from zero to a maximum value $n_{g,\max}'$. Note that ν_0 is a reference frequency chosen such that $n(\nu_0)$ remains constant as n_g' is tuned. We consider a Mach-Zehnder (MZ) interferometer with such a tunable slow-light medium of length L in one arm and a nondispersive reference medium of length L_2 and refractive index n_2 in the other arm. For simplicity, we let $I(\nu) = |E(\nu)|^2$. When the input field has multiple frequency components, the output intensity at each of the two ports of such a MZ interferometer (see Fig. 2) is given by

$$I_{\text{out},\pm} = \frac{1}{4}\int I_{\text{in}}(\nu)|e^{ik[n(\nu_0)+(n_g'\nu'/\nu_0)]L} \pm e^{ikn_2L_2}|^2 d\nu, \tag{2}$$

where $k = 2\pi\nu/c$ is the wave number at frequency ν in

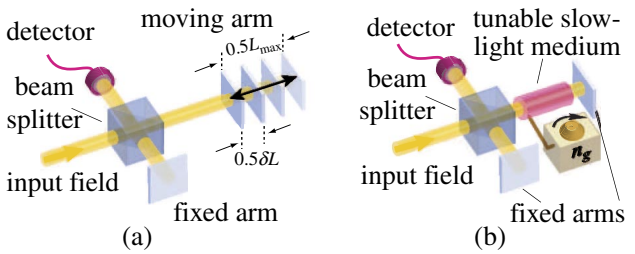

FIG. 1 (color online). Schematic diagrams of (a) a conventional FT interferometer with one moving arm and one fixed arm; (b) a FT interferometer with a tunable slow-light medium in one of the two fixed arms.

 © 2007 The American Physical Society

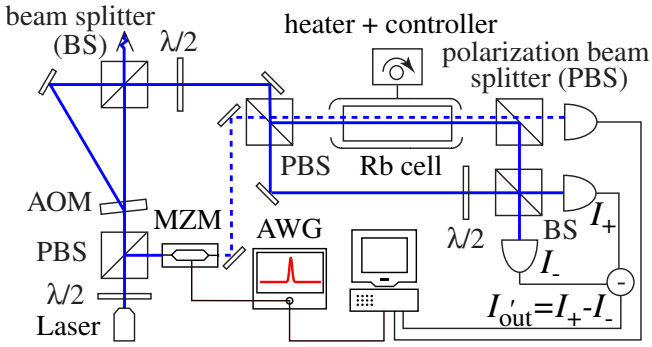

FIG. 2 (color online). Experimental setup of the FT interferometer using a rubidium vapor cell as the slow-light medium.

vacuum. Note that, in practice, both arms also contain other nondispersive media such as beam splitters and air. However, the optical path lengths contributed from these media are assumed to be balanced between the two arms and therefore are not shown in Eq. (2). When the two arms are balanced such that $n_2L_2 = n(\nu_0)L$, one can rewrite Eq. (2) as follows:

$$I_{\text{out},\pm} = \frac{1}{4}\int I_{\text{in}}(\nu)|e^{ik(n'_g\nu'/\nu_0)L} \pm 1|^2 d\nu = \frac{1}{2}I_{\text{in}} \pm \frac{1}{2}\int I_{\text{in}}(\nu)\cos k\frac{n'_g\nu'}{\nu_0}Ld\nu. \quad (3)$$

By subtracting the two outputs, and approximating k by k_0, one obtains the following relation:

$$I'_{\text{out}} \equiv I_{\text{out},+} - I_{\text{out},-} \approx \int I_{\text{in}}(\nu)\cos 2\pi\frac{n'_g\nu'}{c}Ld\nu, \quad (4)$$

where I'_{out} is the modified output that can be directly measured by using a balanced homodyne detection method [17]. Note that, for a pulse with center frequency near ν_0, the relative delay between the two arms of the interferometer is given by

$$\tau_g = \frac{n_gL}{c} - \frac{n_2L_2}{c} = [n_g - n(\nu_0)]\frac{L}{c} = \frac{n'_gL}{c}. \quad (5)$$

We assume that the incident field contains only frequency components that are larger than ν_0, as is in the case of the experiment shown below. In this way, one can obtain the following inverse Fourier transform relation:

$$I'_{\text{out}}(\tau_g) = \int_{-\infty}^{\infty} I_{\text{in}}(\nu_0+\nu')\cos 2\pi\nu'\tau_g d\nu' = \text{Re}\left\{\int_{-\infty}^{\infty} I_{\text{in}}(\nu_0+\nu')e^{i2\pi\nu'\tau_g}d\nu'\right\}, \quad (6)$$

where Re{} denotes the real part. Thus, one can retrieve the input spectrum by applying a Fourier transform to the output intensity scan as a function of τ_g and taking only the result with positive detuning $\nu' > 0$. Note that expression (6) is similar to that of a conventional FT interferometer [e.g., Eq. (11.4) in Ref. [15]], except that in the present case the Fourier conjugate pair is the detuning ν' and the group delay τ_g instead of the absolute frequency ν and the ODT τ.

In the ideal case in which the slow-light medium is lossless, the spectral resolution $\delta\nu$ of such a slow-light FT interferometer is limited by the largest achievable group delay $\tau_{g,\max}$ to $\delta\nu = 1/(2\tau_{g,\max}) = c/(2n'_{g,\max}L)$. Since $n'_{g,\max}$ can be very large when a suitable slow-light medium is used, the spectral resolution of the slow-light FT interferometer can be enhanced by the significant factor of $n'_{g,\max}$ with respect to that of a conventional setup. Alternatively, for a specified spectral resolution $\delta\nu$, the device size can be decreased by a factor of $n'_{g,\max}$.

In many real situations, however, a slow-light medium introduces some frequency-dependent loss. In a tunable slow-light medium of the sort we consider, the ratio between the absorption coefficient α and the relative group index n'_g at each frequency $\nu_0 + \nu'$ remains constant as n'_g is scanned. Thus, for an input of an infinitely sharp spectral line at $\nu_0 + \nu'$, the magnitude of the output I'_{out} will decrease exponentially as n'_g (i.e., τ_g) becomes larger. The Fourier transform of such a decay will result in a Lorentzian-shape spectral line centered at $\nu_0 + \nu'$ with an effective linewidth of $c\alpha/4\pi n'_g$. Thus, the overall spectral resolution near $\nu_0 + \nu'$ is given by

$$\delta\nu(\nu_0+\nu') = \max\left\{\frac{c}{2n'_{g,\max}L}, \frac{c\alpha(\nu_0+\nu')}{2\pi n'_g}\right\}. \quad (7)$$

The total spectral range of such a FT interferometer is given by $\Delta\nu = c/(2\delta n'_gL)$ where $\delta n'_g$ is the step size of the change in n'_g. Note that our slow-light FT interferometer does not require any moving arms, which is advantageous in certain situations in which vibration and translation errors of a moving arm could introduce measurement errors and decrease the SNR.

The theory of Eqs. (1)–(6) can be extended to the more general case in which the slow-light medium has an arbitrary frequency dependence of the refractive index near ν_0 in the form of $n(\nu) = n(\nu_0) + (n'_g/\nu_0)f(\nu')$, where $f(\nu')$ describes the normalized dispersion function near ν_0. In such a case, one can replace ν' by $f(\nu')$ in Eqs. (2)–(6) and obtain the following inverse FT relation:

$$I'_{\text{out}}[\tau_g(\nu_0)] = \text{Re}\left\{\int_{-\infty}^{\infty} I_{\text{in}}(\nu'+\nu_0)e^{i2\pi f(\nu')\tau_g(\nu_0)}d\nu'\right\}, \quad (8)$$

where $\tau_g(\nu_0)$ is the group delay of a pulse centered at ν_0. Note that $\tau_g(\nu_0)$ can be determined from the group delay of a pulse centered at any known frequency $\nu + \nu'$ through the relation $\tau_g(\nu_0) = n'_g(\nu_0)\tau_g(\nu_0+\nu')/n'_g(\nu_0+\nu')$. The Fourier transform of $I'_{\text{out}}[\tau_g(\nu_0)]$ gives first the spectrum I_{in} as a function of $f(\nu')$. When each value of $f(\nu')$ corresponds to a unique value of $\nu_0 + \nu'$ within the spectral range of interest, one can then map out the input spectrum $I_{\text{in}}(\nu_0 + \nu')$ from $I_{\text{in}}(f)$. The spectral resolution

near frequency $\nu_0 + \nu'$ is given by $\delta\nu(\nu_0 + \nu') = \max\{c/[2n'_{g,\max}(\nu_0 + \nu')L], c\alpha(\nu_0 + \nu')/[2\pi n'_g(\nu_0 + \nu')]\}$, where $n'_{g,\max}(\nu_0 + \nu')$ and $\alpha(\nu_0 + \nu')$ are the maximum relative group index and the absorption coefficient of the medium at frequency $\nu_0 + \nu'$, respectively.

We have constructed a slow-light FT interferometer possessing a MZ geometry to demonstrate the properties of our proposed scheme (see Fig. 2). A 10-cm-long rubidium vapor cell is used as the slow-light medium. The tunability of the group index is realized by controlling the temperature and thereby the atomic number density of the cell. A tunable continuous wave (cw) diode laser operating at approximately 780 nm with a linewidth of approximately 100 kHz is used as the primary source. An acousto-optic modulator (AOM) is used to produce a second cw field whose frequency is 80 MHz lower than the primary field. The two fields are combined and used as the input field. Balanced homodyne detection is used to measure the output intensity I'_{out}. For monitoring purposes, a part of the primary laser is directed through a Mach-Zehnder modulator (MZM), which is driven by an arbitrary waveform generator (AWG) to produce a pulse train with 4-ns pulse duration. By measuring the group delay τ_g experienced by such pulses of known frequency in propagating through the vapor cell, the value of n'_g at the primary frequency is obtained.

The refractive index of a rubidium vapor near the D_2 transition lines can be approximated as [18,19]

$$n(\nu) = 1 - \frac{A}{2}\sum_{j=1}^{4}\frac{g_j}{\nu - \nu_j + i\gamma}, \tag{9}$$

where the four terms in the summation correspond to the four major hyperfine transitions of the rubidium D_2 lines [see Fig. 3], g_j and ν_j are the relative peak strength and the frequency center of the jth resonance, respectively, $\gamma \approx 6$ MHz is the homogeneously broadened linewidth of the Rb resonances, and A is a coefficient determined by the atomic number density and the dipole transition moments. The frequency spacing between the centers of neighboring resonances from low to high frequencies are 1.22 GHz, 3.035 GHz, and 2.58 GHz, respectively. The natural abundances of ^{87}Rb and ^{85}Rb are 28% and 72%, respectively; therefore, the relative peak strengths among the four resonances are $g_1{:}g_2{:}g_3{:}g_4 = (5/8) \times 0.28{:}(7/12) \times 0.72{:}(5/12) \times 0.72{:}(3/8) \times 0.28$. The transmission as a function of detuning ν' through the vapor cell at a temperature of approximately 100 °C is plotted in Fig. 3(a). The thick and thin curves show the measured data and the theory of Eq. (9) (with $A = 1.14 \times 10^6$ Hz), respectively. The reference frequency ν_0 is chosen between the resonances of the ^{85}Rb $F = 2 \rightarrow F'$ and ^{87}Rb $F = 1 \rightarrow F'$ transitions so that $n(\nu_0) = 1$ according to Eq. (9). Note that the theory curve for the absorption, which is based on the use of Eq. (9), fits the data very well in the wings of the lines but not near the resonances themselves. This is because Eq. (9) ignores the influence of Doppler broadening and the resulting Gaussian line shape. Since Gaussian line shapes decay much more rapidly in the wings than do Lorentzian line shapes, Eq. (9) accurately describes the atomic response at the frequencies (the gray region in Fig. 3) at which our measurements were performed. The calculated corresponding refractive index n, and group index n_g are plotted in Figs. 3(b) and 3(c), respectively, as functions of ν'.

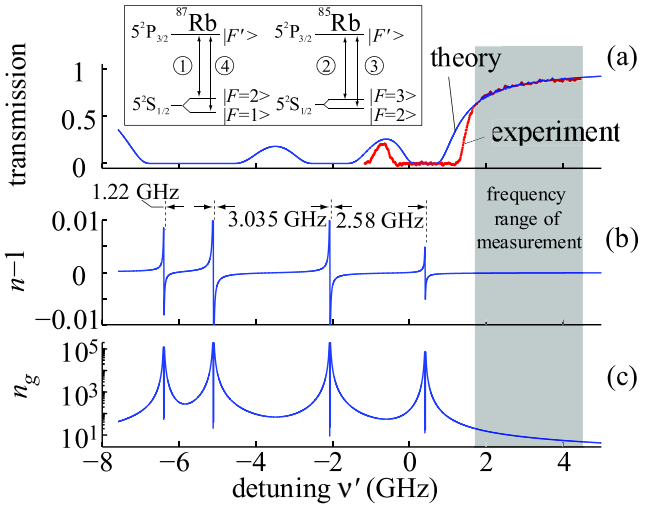

FIG. 3 (color online). (a) Transmission, (b) refractive index n, and (c) group index n_g of the 10-cm-long rubidium vapor cell at the temperature of approximately 100 °C as functions of detuning ν'. The thick curve is the measured transmission, and the thin curves are the fitted theory using Eq. (9). The inset shows the energy levels of the ^{87}Rb and ^{85}Rb D_2 transitions, and the gray region is the frequency region over which the spectral measurement are performed.

The primary frequency of the input field is chosen to be approximately 1.79 GHz higher than the reference frequency ν_0 so that the dispersion model of Eq. (9) can be used. At room temperature, the vapor pressure is practically zero so that $n'_g \approx 0$. As the temperature rises, the atomic number density increases [i.e., A in Eq. (9) increases] and therefore n'_g increases. In the experiment, the pulse delay τ_g and the output intensity I'_{out} are measured simultaneously as the vapor cell is heated from room temperature to approximately 120 °C in a time of approximately 1 min. The maximum group delay is approximately 40 ns, which corresponds to $n'_{g,\max} \approx 120$ at the primary frequency.

Figure 4 shows the experimental data for the output intensity I'_{out} as a function of the group delay τ_g at the primary frequency. The interference pattern clearly shows the beating between the two closely spaced spectral lines. Note that the envelope of I'_{out} is not at a maximum when n'_g approaches zero, which is probably because the phase difference (e.g., due to the coatings on the surfaces of various optical elements in our setup) between the two

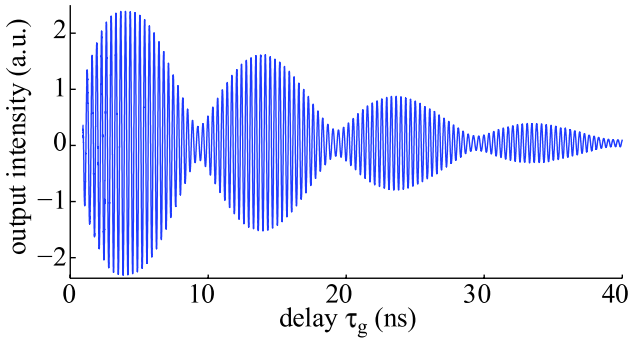

FIG. 4 (color online). Output intensity of the slow-light FT interferometer as a function of the group delay τ_g for an input field of two sharp spectral lines separated by 80 MHz.

arms is not the same for different frequency components of the input field even when $n_g' = 0$.

The input spectrum is retrieved through the FT relation of Eq. (8) and the mapping process described above. The result is plotted as the solid line in Fig. 5. The dotted line is the actual input spectrum, and the dashed line shows the simulated result which is obtained from the calculated I'_{out} using the actual input spectrum, the rubidium model of Eq. (9) and the assumption of a balanced, noise-free interferometer. One sees that the experimental result accurately resolves the position and the profile of the input field. The spectral resolution demonstrated in the experiment is approximately 15 MHz. This value agrees with the simulation result and is limited by the absorption of our slow-light medium. In contrast, a conventional setup with an optical path length difference between the two arms limited to 10 cm could produce a spectral resolution no better than approximately 1.5 GHz. Thus, through use of slow-light methods, we have enhanced the resolution by a factor approximately equal to the maximum group index (100) of our slow-light medium.

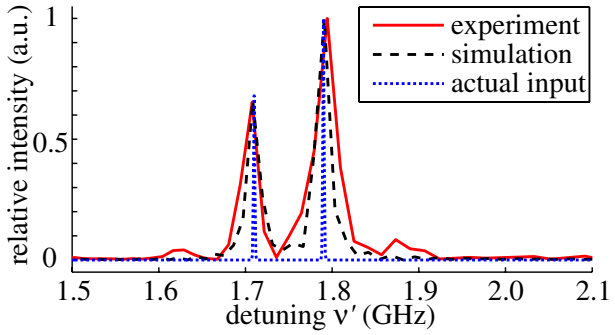

FIG. 5 (color online). Retrieved spectrum of the input field using experimental data (solid line) and simulated data (dashed line) and the actual spectrum of the input field (dotted line). The resolution of a conventional FT interferometer of the same size would be approximately 100 times worse.

In summary, we have proposed and experimentally demonstrated a new type of Fourier transform interferometer that has two fixed arms with a tunable slow-light medium in one arm. We have shown that in such a FT interferometer the spectrum of the input field and the modified output intensity as a function of group delay form a Fourier transform pair. Since the maximum group delay through a slow-light medium can be very large under proper conditions, such a slow-light FT interferometer can provide very high spectral resolution. Moreover, a slow-light FT interferometer might be expected to outperform a conventional FT interferometer by eliminating instabilities and positioning errors associated with the moving arm of a conventional device.

This work was supported by the DARPA/DSO Slow Light program and by the NSF.

*zshi@optics.rochester.edu

[1] R. W. Boyd and D. J. Gauthier, in *Progress in Optics*, edited by E. Wolf (Elsevier Science, Amsterdam, 2002), Vol. 43, pp. 497–530.
[2] S. E. Harris and L. V. Hau, Phys. Rev. Lett. **82**, 4611 (1999).
[3] M. S. Bigelow, N. N. Lepeshkin, and R. W. Boyd, Phys. Rev. Lett. **90**, 113903 (2003).
[4] M. S. Bigelow, N. N. Lepeshkin, and R. W. Boyd, Science **301**, 200 (2003).
[5] G. M. Gehring, A. Schweinsberg, C. Barsi, N. Kostinski, and R. W. Boyd, Science **312**, 895 (2006).
[6] Y. Okawachi *et al.*, Phys. Rev. Lett. **94**, 153902 (2005).
[7] M. Herráez, K. Y. Song, and L. Thévenaz, Appl. Phys. Lett. **87**, 081113 (2005).
[8] P. Ku, C. Chang-Hasnain, and S. Chuang, Electron. Lett. **38**, 1581 (2002).
[9] A. Schweinsberg, N. N. Lepeshkin, M. S. Bigelow, R. W. Boyd, and S. Jarabo, Europhys. Lett. **73**, 218 (2006).
[10] R. M. Camacho, M. V. Pack, and J. C. Howell, Phys. Rev. A **74**, 033801 (2006).
[11] R. M. Camacho, M. V. Pack, J. C. Howell, A. Schweinsberg, and R. W. Boyd, Phys. Rev. Lett. **98**, 153601 (2007).
[12] S. M. Shahriar *et al.*, in *Quantum Electronics and Laser Science Conference (QELS)*, Technical Digest (Optical Society of America, Washington, DC, 2005), paper JWB97.
[13] G. T. Purves, C. S. Adams, and I. G. Hughes, Phys. Rev. A **74**, 023805 (2006).
[14] Z. Shi, R. W. Boyd, D. J. Gauthier, and C. C. Dudley, Opt. Lett. **32**, 915 (2007).
[15] P. Hariharan, *Optical Interferometry* (Elsevier Science, Amsterdam, 2003), 2nd ed., Chap. 11, pp. 173–187.
[16] A. Gomez-Iglesias, D. O'Brien, L. O'Faolain, A. Miller, and T. F. Krauss, Appl. Phys. Lett. **90**, 261107 (2007).
[17] N. Walker and J. Carroll, Electron. Lett. **20**, 981 (1984).
[18] A. Banerjee, D. Das, and V. Natarajan, Opt. Lett. **28**, 1579 (2003).
[19] D. A. Steck, http://steck.us/alkalidata.